

# Back-scattered detection yields viable signals in many conditions

Frederick B. Shipley and Ashley R. Carter\*

Department of Physics, Amherst College, Amherst, Massachusetts 01002, USA

\*[acarter@amherst.edu](mailto:acarter@amherst.edu)

**Abstract:** Precision position-sensing is required for many microscopy techniques. One promising method, back-scattered detection (BSD), is incredibly sensitive, allowing for position measurements at the level of tens of picometers in three dimensions. In BSD the position of a micron-sized bead is measured by back-scattering a focused laser beam off the bead and imaging the resulting interference pattern onto a detector. Since the detection system geometry is confined to one side of the objective, the technique is compatible with platforms that have restricted optical access (*e.g.* magnetic tweezers, atomic force microscopy, and microfluidics). However, general adoption of BSD may be limited according to a recent theory [Volpe *et al.*, *J. Appl. Phys.* **102**, 084701, 2007] that predicts diminished signals under certain conditions. We directly measured the BSD response while varying the experimental conditions, including bead radius, numerical aperture, and relative index. Contrary to the proposed theory, we find that all experimental conditions tested produced a viable signal for atomic-scale measurements.

©2012 Optical Society of America

**OCIS codes:** (180.0180) Microscopy; (180.6900) Three-dimensional microscopy; (120.0120) Instrumentation, measurement, and metrology; (180.5810) Scanning microscopy.

---

## References and links

1. S. C. Jordan and P. C. Anthony, "Design considerations for micro- and nanopositioning: leveraging the latest for biophysical applications," *Curr. Pharm. Biotechnol.* **10**(5), 515–521 (2009).
  2. S. O. R. Moheimani, "Invited review article: accurate and fast nanopositioning with piezoelectric tube scanners: emerging trends and future challenges," *Rev. Sci. Instrum.* **79**(7), 071101 (2008).
  3. R. Puers, "Capacitive sensors - when and how to use them," *Sens. Actuat. A* **37–8**, 93–105 (1993).
  4. A. D. Kersey, M. A. Davis, H. J. Patrick, M. LeBlanc, K. P. Koo, C. G. Askins, M. A. Putnam, and E. J. Friebele, "Fiber grating sensors," *J. Lightwave Technol.* **15**(8), 1442–1463 (1997).
  5. J. J. Dosch, D. J. Inman, and E. Garcia, "A self-sensing piezoelectric actuator for collocated control," *J. Intell. Mater. Syst. Struct.* **3**(1), 166–185 (1992).
  6. A. R. Carter, G. M. King, and T. T. Perkins, "Back-scattered detection provides atomic-scale localization precision, stability, and registration in 3D," *Opt. Express* **15**(20), 13434–13445 (2007).
  7. M. E. J. Friese, H. Rubinsztein-Dunlop, N. R. Heckenberg, and E. W. Dearden, "Determination of the force constant of a single-beam gradient trap by measurement of backscattered light," *Appl. Opt.* **35**(36), 7112–7116 (1996).
  8. U. F. Keyser, J. van der Does, C. Dekker, and N. H. Dekker, "Optical tweezers for force measurements on DNA in nanopores," *Rev. Sci. Instrum.* **77**(10), 105105 (2006).
  9. J. H. G. Huisstede, K. O. van der Werf, M. L. Bennink, and V. Subramaniam, "Force detection in optical tweezers using backscattered light," *Opt. Express* **13**(4), 1113–1123 (2005).
  10. G. M. King, A. R. Carter, A. B. Churnside, L. S. Eberle, and T. T. Perkins, "Ultrastable atomic force microscopy: atomic-scale stability and registration in ambient conditions," *Nano Lett.* **9**(4), 1451–1456 (2009).
  11. G. Volpe, G. Kozyreff, and D. Petrov, "Backscattering position detection for photonic force microscopy," *J. Appl. Phys.* **102**(8), 084701 (2007).
  12. W. Denk and W. W. Webb, "Optical measurement of picometer displacements of transparent microscopic objects," *Appl. Opt.* **29**(16), 2382–2391 (1990).
  13. K. Visscher, S. P. Gross, and S. M. Block, "Construction of multiple-beam optical traps with nanometer-resolution position sensing," *IEEE J. Sel. Top. Quantum Electron.* **2**(4), 1066–1076 (1996).
  14. F. Gittes and C. F. Schmidt, "Interference model for back-focal-plane displacement detection in optical tweezers," *Opt. Lett.* **23**(1), 7–9 (1998).
-

15. A. Pralle, M. Prummer, E. L. Florin, E. H. K. Stelzer, and J. K. H. Hörber, "Three-dimensional high-resolution particle tracking for optical tweezers by forward scattered light," *Microsc. Res. Tech.* **44**(5), 378–386 (1999).
  16. A. R. Carter, G. M. King, T. A. Ulrich, W. Halsey, D. Alchenberger, and T. T. Perkins, "Stabilization of an optical microscope to 0.1 nm in three dimensions," *Appl. Opt.* **46**(3), 421–427 (2007).
  17. A. R. Carter, Y. Seol, and T. T. Perkins, "Precision surface-coupled optical-trapping assay with one-basepair resolution," *Biophys. J.* **96**(7), 2926–2934 (2009).
- 

## 1. Introduction

Precision position-sensing is important in microscopy, semiconductor fabrication, and robotic motion control [1, 2]. Commonly in these applications movements on the nanometer-scale are accomplished by voltage-controlled piezo actuators or flexures, which are prone to hysteresis and drift and necessitate position sensing. Positional readouts of the piezo elements can be measured by capacitive [3], interferometric [4], or strain [5] position sensors. Such read outs are most effective if they are performed at points local to the system under study.

The ultimate limit of the position sensor is set by the underlying signal, which has two general guidelines. The first is that the signal should be monotonic, preferably linear, over a desired range. The second guideline is that the slope of the linear region, or sensitivity, should provide enough resolution to allow for position sensing at the desired level. Here we are interested in an atomically precise, interferometric position-sensing technique: back-scattered detection (BSD).

BSD allows for atomic-scale resolution [6], and for laser position-sensing in experiments that are geometrically constrained. In BSD a focused laser beam is scattered off a micron-sized bead or other scattering structure (Fig. 1). The back-scattered light and the reflected beam are collected by the objective and interfere in the back focal plane. The signal in BSD is set by this interference pattern, which is imaged onto a detector behind the objective. If the bead moves, the interference pattern changes, and the detector measures a corresponding change in voltage. Using this technique, motion at the level of tens of picometers has been detected in three dimensions [6]. Historically, BSD has been used in optical trapping experiments to measure the position of an optically trapped bead [7–9]. However, since BSD optics are all on one side of the objective, the detection scheme can be coupled to applications with limited access, including atomic force microscopy [10]. Given the atomic scale resolution and optical conciseness of BSD, we envision its incorporation into many exciting precision measurement platforms, including lithography, magnetic tweezers, and microfluidics.

However, recent theoretical work [11] predicts that in some conditions the back-scattered signal will be vanishingly small, limiting the applicability of BSD. In this theory the intensity at the detector is calculated by assuming Mie-Debye scattering and a first order interference in the back-focal-plane of the objective. The model also assumes that the reflected beam from the surface is less intense than the transmitted light, such that the response is solely due to the scattered electric field. Given these assumptions, the authors find that the BSD response varies in a complex way with numerical aperture and bead size. For example, as bead radii is increased from 100 nm to 2000 nm the BSD response oscillates between a positive and negative sensitivity, and passes through zero for certain radii (*e.g.* 1000 nm). While the theory is rooted in previous observations of BSD signals from trapped beads [9], it has yet to be experimentally tested for use in position-sensing applications. If the theoretical predictions are valid, then back-scattered signals would be too small in certain conditions to make BSD practical.

Additionally, the theory finds that BSD signals should be inferior to signals obtained using forward-scattered detection, FSD, and would limit the usefulness of BSD. In FSD the scattered laser deflection and the transmitted beam are both collected, and their interference pattern is projected onto a detector in the forward position [12, 13]. In the recent theory [11], forward scattered signals are calculated by assuming Mie-Debye scattering and a first order interference between the transmitted and forward-scattered light. The predicted shape of the

forward-scattered signal follows the experimentally determined response [14, 15], and, interestingly, is similar to a theoretical curve that assumes the bead acts as a Rayleigh scatterer [14, 15]. Comparison of the theoretical BSD and FSD signals shows that the FSD response has a slightly larger range (a change of  $\sim 100$  nm) and a 100-fold greater amplitude [11]. This decrease in signal strength and range for BSD could negate any decrease in noise that the optical conciseness of the setup affords [6]. Furthermore, the theoretical FSD signal is predicted to increase with bead radius, in contrast to the theoretical BSD response that changes sign with bead radius [11]. Thus, there is a need for an experimental study of BSD signals to test the predictions made by the theoretical model and address the limitations of BSD position sensing.

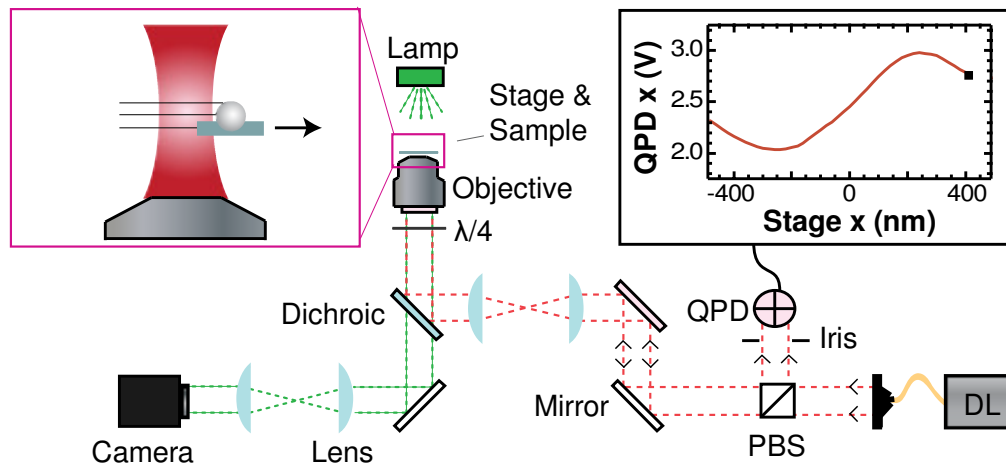


Fig. 1. Optical schematic for back-scattered detection (BSD). In BSD a laser is coupled into a microscope and the focused beam back-scatters off a bead in the sample plane (*Inset*). The diode laser (DL,  $\lambda = 945$  nm, *red dashed line*) is launched from a fiber to obtain a Gaussian mode. The combination of the polarizing beam splitter (PBS) and quarter-wave plate ( $\lambda/4$ ) act as an optical isolator for highly efficient BSD. The quadrant photodiode (QPD) measures the scattered light. As the bead is moved through the laser in  $x$  by the stage, the scatter changes and the quadrant photodiode records the BSD signal. Here we display the signal in  $x$  that has been normalized by the total intensity on the QPD. Data is from a 300-nm-radius bead in water.

As a preliminary experiment, we measured lateral BSD signals from a bead attached to a cover slip and compared these signals with FSD signals. We first measured the signal from a 300-nm-radius bead in water (Fig. 1). When we fit the curve with a derivative of a Gaussian the width we obtained was 340 nm, similar to the previously measured width of 330 nm for FSD signals [15]. In addition, the BSD sensitivity of a 200-nm-radius bead without post amplification is 5.5 mV/nm, the same order of magnitude as the FSD signal for a 200-nm-radius bead using similar electronics [16]. Contrary to the theoretical prediction, we do not see a drop in the sensitivity of the lateral BSD response by a factor of 100 in comparison to FSD, nor a decrease in the linear detection range. This disagreement of the theory with the preliminary data necessitated a closer look into the theoretical predictions.

We perform such a study and investigate the applicability of BSD in precision position-sensing experiments. As a preface to these results, we first describe two experimental tactics to increase BSD sensitivity and record optimal signals. The first is to use an iris to isolate the back-scattered light from the bead (Section 3.1). The second is to select the appropriate axial position (Section 3.2). Using the optimal signal obtained with these measurements we determine the lateral BSD sensitivity as a function of bead radius, relative index, and numerical aperture (Section 3.3). We do not observe the theoretically predicted outcome; instead we see that the BSD signals are similar to FSD signals, possibly due to a measurable

reflection from the glass-medium interface that is not taken into account in the proposed BSD theory [11].

Furthermore, for all of the tested conditions, we record signals capable of atomic-scale resolution, indicating the broad applicability of BSD for position-sensing. We anticipate the integration of BSD into many applications that require precision sensitivity and control.

## 2. Materials and methods

### 2.1 Experimental apparatus

The experimental apparatus for BSD is optically concise and allows for ease of implementation (Fig. 1). In BSD a laser is coupled into an objective and focused to a diffraction-limited spot. The focused beam back-scatters off a bead or other scattering structure, and the objective collects both the back-scattered and reflected light. The interference is projected on to a detector behind the objective. Thus, all the experimental optics are placed on one side of the sample, removing the need for optics mounted after the condenser lens as in FSD [17]. This geometric freedom allows detection of particles in conjunction with physically constraining systems, such as patch clamp experiments, scanning probe microscopes, or magnetic tweezers.

We built a system designed for efficient collection of the BSD signal, as was previously described [6]. In this system, a diode laser ( $\lambda = 945$  nm in air, Lumics) is launched from a single-mode fiber with a collimating lens to create a Gaussian mode. The diode laser is current-controlled using custom electronics and was run at three different current levels: 100 mA, 160 mA, and 300 mA. The selection of the current is important for obtaining the best lateral and axial signals. Coupling of the laser into the microscope is achieved with a gimbal-mounted mirror, a telescopic lens system, and a dichroic mirror. The dichroic mirror reflects the laser into the microscope and transmits the visible light of the lamp to the camera for imaging. The lens system between the gimbal mirror and the objective serves two purposes. The first purpose is to image the gimbal mirror to the back aperture of the objective, creating independent beam steering in the sample plane by pure rotations of the mirror. The second purpose is to set the beam diameter to  $\sim 5$  mm to allow for a tightly focused laser spot. Focusing of the laser and collection of the BSD signal was implemented with a high numerical aperture objective (Leica, 100X, oil immersion, numerical aperture = 1.35). We detected the back-scattered signal from a bead on a cover slip using a quarter-wave plate, a polarizing beam splitter, and a quadrant photodiode (YAG 444-4A, PerkinElmer Optoelectronics). The combination of the quarter-wave plate and the polarizing beam splitter act to optically isolate the back-reflected light. The quarter-wave plate was tilted to reduce the back reflection. Using these optics we achieve a back-scattered signal of 190  $\mu$ W or 2% of the laser power input into the objective. (This measurement was taken at 100 mA with a sample of 480-nm-radius latex beads in air.) Higher collection efficiencies can be achieved with a higher numerical aperture objective [6].

We highlight that we have added an iris to the system to isolate the central portion of the interference pattern at the detector. Selection of this region increases the sensitivity as shown in Section 3.1. Previous implementations of BSD have used various detection schemes including lensing through a pinhole [8] and overfilling the quadrant photodiode [7]. Though not explicitly stated, these implementations may also select the central back-scattered portion. Isolation of this region is important to obtain the most sensitive lateral signals by minimizing the extraneous reflected light.

### 2.2 Data acquisition and analysis

Data was acquired from the quadrant photodiode and processed in LabView for automated measurement and analysis. The lateral motion ( $x$ ,  $y$ ) of the bead relative to the laser was deduced from the normalized intensity difference on the quadrant photodiode [14]; for

example, the voltage in  $x$  was given by the voltage of the right two quadrants minus the voltage of the left two quadrants divided by the total voltage on all four quadrants. The axial motion ( $z$ ) was deduced from the total voltage [15]. To improve resolution for precision positioning, voltages were amplified from the normalized difference signals. After antialias filtering (1.2 kHz), the lateral and axial voltages were digitized with a 20-volt range, 12-bit data acquisition card (M-series, National Instruments) at 4 kHz. To measure BSD response curves of voltage vs. position we moved a closed-loop, piezo-electric stage (Tritor, Piezo Systems Jena) to the desired position and averaged 100 raw data points. The sensitivity in V/nm was obtained by fitting a line to the linear region of the curve. Traces were smoothed with a binomial filter for presentation.

### 2.3 Varying experimental conditions

We measured the BSD response in multiple experimental conditions. To vary bead radii we attached different sized, commercially available latex beads (IDC latex beads, Invitrogen) to an epoxy-rigidified sample chamber [6]. The fluid in the sample chamber sets the index of refraction of the medium,  $n_{med}$ , and thus, the relative index,  $m$ , as given by  $m = n_{object} / n_{med}$ , where  $n_{object}$  is 1.59. The medium index at 590 nm for the fluids that were used are as follows: air (1.00), code 126 (1.26; Cargille), water (1.33), and refractive index liquid (1.30 and 1.40; Cargille). To vary the numerical aperture of the objective we placed an iris at the entrance pupil. Closing the aperture decreased the effective diameter of the lens, and therefore, the numerical aperture. We approximate the new numerical aperture using the following formula for a thin lens:  $NA = n \sin(\tan^{-1}(D/2f))$ . Here  $NA$  is the numerical aperture,  $D$  is the effective diameter of the lens given by the iris opening,  $f$  is the focal length, and  $n$  is the refractive index. Thus, we were able to vary the bead radius, relative index, and numerical aperture to observe how the BSD sensitivity changes with these experimental parameters.

## 3. Results

### 3.1 Isolation of the central back-scattered light increases lateral BSD sensitivity

Isolating the central section of the back-scattered interference pattern is necessary to obtain the best lateral BSD sensitivity. The interference pattern is a superposition of light back-scattered by the bead and light reflected from the sample surface—the interface between the glass cover slip and the sample medium. As the bead is scanned laterally through the laser the central section of the interference pattern changes, while the outer portion, due solely to the reflection at the sample surface, stays constant. By selecting the central region of the interference pattern with an iris, we eliminate the offset voltage on the quadrant photodiode caused by light from the surface and increase the BSD signal.

We demonstrate this process by isolating the central, back-scattered light from a 480-nm-radius bead in air [Fig. 2(a)]. As the iris closes and blocks the outer region, the light reflected from the glass-air boundary is reduced, effectively decreasing the background. The central back-scattered signal from the bead remains unchanged, and therefore, the normalized difference between the left and right quadrants increases, creating a larger BSD response. To quantify the increase, we fit the linear portion of the curve and measured the sensitivity. The change in sensitivity from the iris in the fully open position (diameter = 7.5 mm) to almost closed (diameter = 2.1 mm) is 3.1 mV/nm to 14.6 mV/nm, a factor of 4.7. As expected, the monotonic region of the curve in both cases has a range of 500 nm, indicating that the range of the lateral signal is not affected by the iris. We note that the enhancement in the lateral signal is concurrent with a decline in the axial signal. The iris blocks some of the light, causing a decrease in the axial range from 3000 nm to 1500 nm [Fig. 2(b)]. Thus, selection of the central back-scattered region using the iris causes a trade-off in axial signal for an increase in lateral BSD sensitivity.

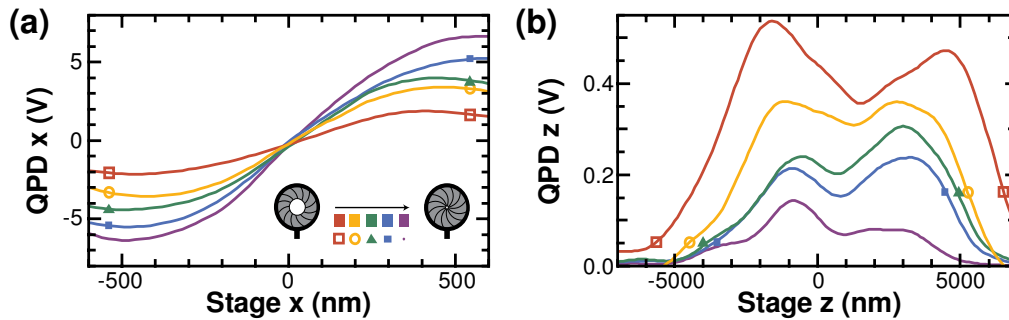


Fig. 2. Isolation of the central back-scattered region leads to increased lateral BSD sensitivity. (a) *Inset*. An iris in front of the detector isolates the central region. As the iris is closed, the slope of the lateral BSD response increases for 480-nm-radius beads in air. Colors go from red to purple as the iris is closed. Curves also denoted by symbols as shown. (b) Response of the BSD axial signal as the iris is closed. Color and symbols same as in (a). Traces offset for clarity.

Additionally, there are two more caveats in using the iris to increase the lateral sensitivity. The first caveat is that while we find that iris position is important when using 480-nm-radius beads in air, not all experimental conditions require the iris to increase the signal. If the reflection from the glass-medium interface is small compared to the back-scattered signal, then the iris is essentially blocking light that is relatively dim, and is not necessary. The second caveat is that the iris can be used at any position, from fully open to fully closed, to give a range of sensitivities. The question then becomes which position to use. From a position-sensing perspective, the iris position that maximizes lateral sensitivity might be the best choice (optimally closed), or the iris position that maximizes the total light falling on the detector might be the best choice (fully open). From a theoretical perspective, perhaps the iris position that selects the light back-scattered from the bead without any clipping is the best choice (closed without clipping). We note that the optimally closed position is achieved when the iris significantly clips the back-scattered light from the bead, such that optimally closed and closed without clipping are two different cases. We report data in the closed without clipping configuration unless otherwise indicated. Given these caveats, we find that the lateral BSD sensitivity can be experimentally increased by selecting the central back-scattered light with an iris.

### 3.2 Axial position changes the sign and magnitude of the lateral BSD sensitivity

The lateral BSD sensitivity is exquisitely sensitive to axial position. Both the sign and amplitude of the lateral signal will change as the axial position is varied. Therefore, choosing an axial position for a given experiment is necessary.

To choose an axial setpoint, we first limit the choice of position to regions where the axial signal has a nonzero slope to accommodate position sensing in  $z$ . We observe that the axial signal is the sum of the reflected light from the glass-medium interface and the back-scattered light from the bead. These two components have curves that correspond to a singular maximum and a derivative of a Gaussian, respectively. Their sum, the axial BSD response, varies depending on the amplitudes of the two components [Fig. 3(a)]. When the back-scattering by the bead is minimal compared to the reflection from the glass-medium interface (*e.g.* when the bead radius is  $\leq 100$  nm in air), then the axial signal has a singular maximum. When the back-scattering is larger (*e.g.* as for larger bead radii of  $\geq 200$  nm in air), then the axial signal appears as a curve with two maxima. Given these curves, we find three linear regions: *A*, *B*, and *C* that would yield viable axial signals.

We then measure the lateral BSD sensitivity in each of the three regions to determine the optimal axial position. An intensity plot of lateral sensitivity in air as a function of position in  $z$  shows a maximum slope in region *A* [Fig. 3(a)]. Furthermore, a plot of the maximum lateral

sensitivity in each of the three regions as a function of bead size shows again that the maximum lateral sensitivity occurs in region A [Fig. 3(b)]. For comparison, the magnitude of the axial sensitivity in all three regions was fairly constant at 0.02-0.03 mV/nm [Fig. 3(c)]. Given this data, we denote the optimal axial position as the location in region A that produces the maximum lateral sensitivity. In this work we use this optimal axial position for all other measurements, unless otherwise noted.

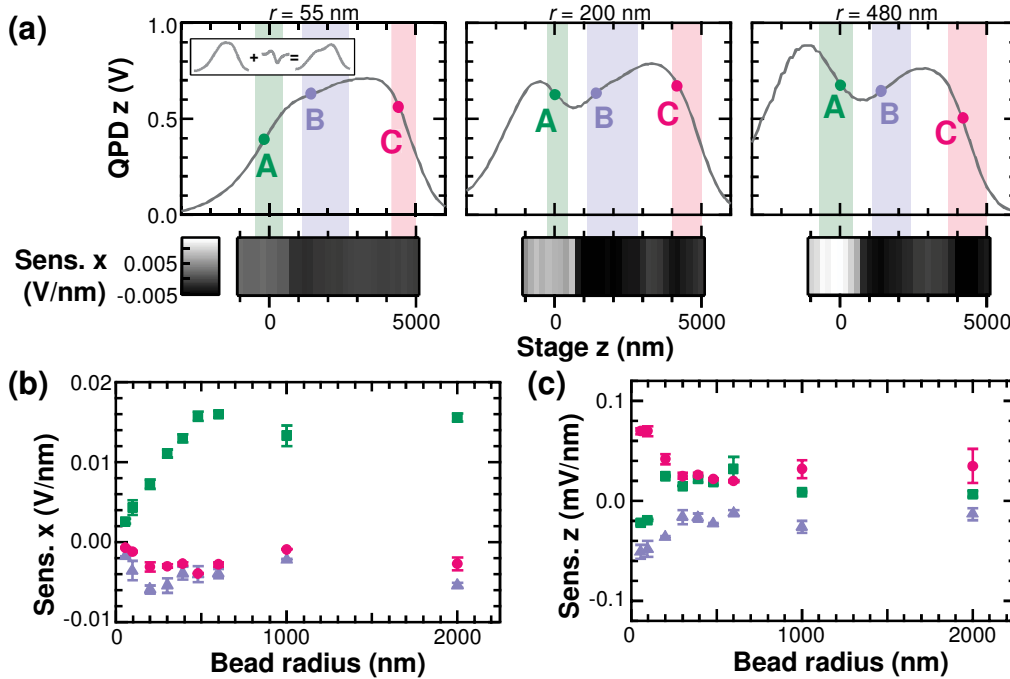


Fig. 3. Selection of the optimal axial position maximizes lateral BSD sensitivity. (a) *Inset*. The axial BSD response is the sum of the voltage from the reflected light off of the glass-medium interface, which has a singular minimum, and the back-scattered light off of the bead, which is the derivative of a Gaussian. *Left, center, and right* axial signals correspond to bead radii of 55 nm, 200 nm, and 480 nm, respectively. Lateral BSD sensitivity (Sens. x) as a function of position in  $z$  (200 nm increments) is displayed as an intensity plot below each graph. There are three regions A (green), B (light purple), and C (magenta) where the axial BSD signal is linear. The  $z$  position that produces the maximum lateral sensitivity for a region is denoted by a point. The lateral, (b), and axial, (c), BSD sensitivities at points A, B, and C for beads of varying radii in air. Color scheme same as in (a).

Interestingly, the sign of the BSD lateral sensitivity is a function of axial position. We observe that the lateral signals are positive at position A and negative at positions B and C. This sign change is possibly explained by the inversion due to passing through the laser focus from position A to C. We note that we do not observe a change in the sign of the BSD sensitivity with bead radius, as previously reported [9]. This may be due to experimental differences as the previous measurement used an optically trapped bead and a different technique to collect the back-scattered signal.

### 3.3 Lateral BSD signals vary with bead size, relative index, and numerical aperture

After determining how the iris position and axial location affect the sensitivity of the lateral signals, we wanted to test how these signals vary with bead radius, relative index, and numerical aperture.

We observe that the lateral BSD sensitivity increases with bead radius in water, and then levels off [Fig. 4]. A line was fit to the data for radii  $\leq 480$  nm. Similar data is shown for

signals in air in Fig. 3(b). In both cases we do not observe an oscillating sensitivity as predicted by theory [11], nor a change in sign as has been previously measured [9]. In addition, the sensitivity does not vary as the cube of the radius for small bead sizes as the Rayleigh scattering regime might predict [14]. We instead find a linear relationship between sensitivity and bead radius for bead radii of < 500 nm.

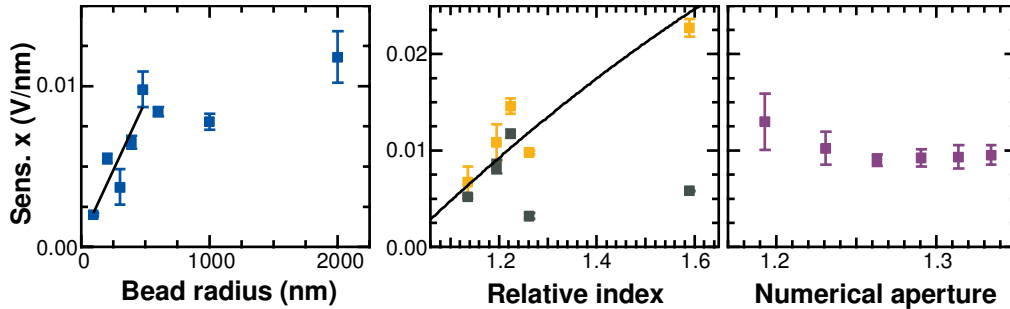


Fig. 4. Lateral BSD sensitivity varies with bead radius, numerical aperture, and relative index. *Left.* As bead radius increases the BSD sensitivity in water (blue) increases and then levels off. Linear fit for bead radii  $\leq 480$  nm (black). *Center.* As relative index increases a spherical scattering particle in the Raleigh regime would produce an increased lateral sensitivity due to an increase in polarizability (black, function in main text). Data for 480-nm-radius beads with the iris fully open (gray) shows a drop in sensitivity, while the iris in the optimally closed position (yellow) follows the prediction. *Right.* As the numerical aperture decreases, the sensitivity for 480-nm-radius beads in water remains constant (purple).

We also measured lateral BSD sensitivity as a function of relative index and found that the maximum sensitivity increases as the polarizability of the bead increases [Fig. 4]. To vary the relative index we changed the medium inside the chamber using refractive index liquid (nominal index of 1.40, 1.30, and 1.26), water, and air. Previous measurements [6] that varied the relative index by changing the index of the scattering object found that the sensitivity,  $S$ , increased with polarizability,  $\alpha$ , as might be expected for spherical particles in the Rayleigh regime [14]. Similarly, the data in our experiment might follow the function:  $S = S_0 \alpha / \alpha_0$ , which assumes the ratio of the sensitivities is equal to the ratio of the polarizabilities. In this function  $S_0$  and  $\alpha_0$  are fit reference values, and the polarizability depends on bead volume,  $V$ , and relative index:  $\alpha = 3V(m^2 - 1) / [4\pi(m^2 + 2)]$ . When we measured lateral BSD signals from 480-nm-radius beads taken with the iris in the fully open position (gray), we noticed a drop in sensitivity at a relative index of 1.26. If we set the iris to the optimally closed position (yellow) instead, then the sensitivity increased with relative index as expected. The drop in sensitivity must then be due to an increase in background light on the quadrant photodiode from the surface reflection relative to the back-scattered light from the bead. This makes sense as a medium change from water to air would increase the surface reflectivity  $[R = (n_{\text{glass}} - n_{\text{medium}})^2 / (n_{\text{glass}} + n_{\text{medium}})^2]$  ten-fold, while polarizability would only increase three-fold. By removing the background light on the quadrant photodiode, we see that the lateral BSD sensitivity increases with polarizability, similar to the theoretical prediction for FSD signals [14].

Finally, we tested the dependence of the lateral BSD sensitivity on the effective numerical aperture of the objective [Fig. 4]. To change the effective numerical aperture we used a second iris at the entrance pupil of the objective to limit the diameter of the lens. As one might expect, we noticed that as the iris diameter decreased the intensity of the back-scattered light diminished without affecting the shape of the interference pattern at the detector. Using this configuration we collected data using 480-nm-radius beads in water. We observe that as the effective numerical aperture of the objective decreases, the signal stays relatively constant.



At the smallest numerical aperture measured there is an increase in sensitivity; however this is most likely artificial. As the iris is closed the amount of light reaching the quadrant photodiode becomes small. Because the signal is normalized by the total intensity there is an effective division by zero that tends to increase both the signal and noise. As the iris is closed further, light collection is decreased and we are unable to measure a signal. We conclude that experimentally the numerical aperture needs to be above a threshold value (here numerical aperture = 1.2), set by the detector threshold and incident laser power, to produce a signal. Above this threshold value, lateral BSD sensitivity is independent of numerical aperture.

Importantly, in all of the conditions tested we find viable signals for atomic-scale measurements. The smallest lateral sensitivity we record is 2 mV/nm. If we apply a 10-fold post amplification and use an 18-bit data acquisition card with a 20-V range, as was done previously [6], then this yields a resolution of 4 pm/bit. However, this resolution is only possible if the noise in the experiment (optical trap, scanning probe microscope, etc.) is equally low over the time period for the measurement. Currently, the lateral BSD positional stability is limited to 10 pm over the bandwidth 0.1-1 Hz [6]. We therefore find viable BSD signals in a variety of experimental conditions for atomic-scale measurements.

#### 4. Conclusion

While recent BSD theory [11] predicts a vanishingly small signal in certain conditions, we find that BSD signals are viable for atomic-scale measurements in many situations. We first describe two experimental procedures that optimize the BSD signal: selecting the back-scattered signal with an iris and choosing the optimal axial position. With these optimal settings we measure the BSD response while varying bead radius, numerical aperture, and relative index. Contrary to the proposed theory, we find that the smallest BSD sensitivity measured still has the potential for atomic-scale resolution. The BSD sensitivity also does not oscillate with bead radius as predicted. Instead, the signal increases with bead radius similar to the FSD prediction [11]. Thus, we conclude that BSD signals provide a viable alternative to FSD signals, with the added attribute of optical conciseness.

Given our experimental measurements we propose that the theoretical model [11] for BSD should be modified to include a reflection from the sample surface. In the theory the BSD response is solely due to the light back-scattered by the bead, while the FSD response is a sum of both the light forward-scattered by the bead and the transmitted light. Experimentally, we find that the light reflected at the sample surface is comparable to the light back-scattered by the bead. We therefore assume that the reflected beam might be analogous to the transmitted beam in FSD, and would account for the similarities between FSD and BSD. Currently, the theory indicates that this ~1% reflection at the surface is negligible compared to the intensity of the transmitted beam, and accounts for the proposed differences between FSD and BSD [11]. It is then interesting that our data indicate that this small surface reflection is significant. We propose that the theory be updated with a term for the surface-reflected light to determine if our predictions are correct.

In addition, our experimental results may not be at odds with a previous result which finds that the sign of the BSD signal switches as bead radius is increased from 225 nm to 535 nm [9]. First, it is possible that the axial position in the previous data was not optimized as we have described. As the sign of the lateral signal is sensitive to axial position this might account for the difference. Second, it is possible that the previous experiment collected a back-scattered signal with a relatively small reflection from the glass-medium interface. In this case we might expect the sign to change as predicted by the theoretical model [11]. As the total light falling on the QPD is an order of magnitude lower than our measurements, it seems likely that the surface reflection is much smaller. If indeed the reflection at the surface is negligible, then the two experimental measurements would be complementary, further necessitating the expansion of the theoretical model to include a term for the reflection at the sample surface.

As we do not reproduce the expected results proposed by the theory [11], one might argue that the theory is correct and our results are not applicable. We argue that this is not the case. In the theory an optically trapped bead is modeled as a sphere in a homogenous medium, and the reflection from the sample surface is ignored. If the reflection is truly insignificant we would expect our BSD signals from beads attached to the cover slip to be exactly the same as optically trapped beads. On the other hand, if the surface reflection is significant then it should be included in the theory. Thus, our system is able to effectively test one of the underlying assumptions of the theory while also measuring the applicability of BSD in position sensing.

We conclude that BSD signals are sensitive enough to detect atomic-scale signals in a variety of conditions, contrary to the proposed theory [11]. We envision that BSD will be useful in a number of position sensing applications that require precision measurements but are limited in optical geometry.

### **Acknowledgments**

The authors would like to thank Tom Perkins for equipment, Carl Sauer and Norm Page for custom electronics, and Bob Cann and Misha Coggeshall-Burr for custom machining. This work was supported by Amherst College and a Howard Hughes Medical Investigator undergraduate fellowship (FBS).